Article

Not peer-reviewed version

Characteristics and Driving Mechanisms of Coastal Wind Speed During Typhoon Season: A Case Study of Typhoon Lekima

Lingzi Wang , Aodi Fu , Bashar Bashir , Jinjun Gu , Haibo Sheng , Liyuan Deng , Weisi Deng , Karam Alsafadi *

Posted Date: 3 June 2024

doi: 10.20944/preprints202406.0100.v1

Keywords: Beast; Hurst index; Typhoon Lekima; wind speed characteristics; driving mechanism

Article

Characteristics and Driving Mechanisms of Coastal Wind Speed During Typhoon Season: A Case Study of Typhoon Lekima

Lingzi Wang [1], Aodi Fu [2], Bashar Bashir [3], Jinjun Gu [2], Haibo Sheng [1], Liyuan Deng [1], Weisi Deng [1] and Karam Alsafadi [4,*]

[1] Power Dispatching and Control Center of China Southern Power Grid, Guangzhou, 510000, China; wanglz2@csg.cn (L.W.); shenhb1@csg.cn (H.S.); dengly3@csg.cn (L.D.); dengws@csg.cn (W.D.)
[2] School of Geographical Sciences, Nanjing University of Information Science & Technology, Nanjing, 210044, China; 20211210006@nuist.edu.cn (A.F.); 18767305830@163.com (J.G.)
[3] Department of Civil Engineering, College of Engineering, King Saud University, P.O. Box 800, Riyadh 11421, Saudi Arabia; bbashir@ksu.edu.sa
[4] Key Laboratory of the Ministry of Education for Coastal and Wetland Ecosystems, College of Environment and Ecology, Xiamen University, Xiamen, Fujian 361102, China
* Correspondence: karam.alsafadi@xmu.edu.cn

Abstract: The development and utilization of wind energy is of great significance to the sustainable development of China's economy and the realization of the goal of "dual carbon". Under the typhoon system, the randomness and volatility of wind speed become an important basis for affecting the energy efficiency utilization and design of wind turbines. Therefore, based on wind speed and wind direction data at 10m, 30m, 50m and 70m heights of a wind power tower in Yancheng, Jiangsu Province, this paper analyzes the change characteristics of wind speed and wind direction by using BFAST method and Hurst index. Based on typhoon body data, topographic data and mesoscale system wind direction data, the causes of the occurrence and development of wind speed and wind direction of wind tower are further analyzed, and a conclusion is drawn: (1) In BEAST method, there are 5, 5, 6 and 6 change points at the height of 10m, 30m, 50m and 70m respectively. Among them, the change points at the height of 10m, 30m and 50m all change before and after node 325, and the change time point at the height of 70m is inconsistent with other heights. Hurst index results show that the inconsistency at 70m altitude is stronger than that at other altitudes. (2) The wind direction sequence at 10m, 30m, 50m and 70m altitude is fitted by stages, and the direction of wind direction is SE-E-SE-SW-W-NW, where, At the height of 70m, the deviation of the fitting trend line from other altitudes is larger in the wind speed strengthening stage and weakening stage. (3) The wind speed at the height of 10m and 70m has different response degrees to the typhoon body. The correlation between the wind speed and the distance between the wind measurement tower and the typhoon near the center is stronger at the height of 10m than at the height of 70m. The surface type and the wind direction of the mesoscale system also have certain effects on the wind speed and direction. In this paper, the change characteristics and influencing factors of wind speed and direction of wind tower are studied, which provides methods and theoretical support for the study of short-term wind speed when typhoon passes through, and provides reliable support for the selection of wind power forecast indicators and the selection and design of wind turbines under extreme gale weather systems.

Keywords: Beast; Hurst index; Typhoon Lekima; wind speed characteristics; driving mechanism

 doi:10.20944/preprints202406.0100.v1

1. Introduction

Wind is one of the renewable resources, and the rational development and utilization of wind energy are of great significance to the sustainable development of China's economy and the realization of the "double carbon" goal [1]. Due to the influence of weather systems such as underlying surface characteristics, temperature, pressure, and circulation, wind speed is characterized by randomness and volatility in a short period, which causes the power generation of wind turbines to fluctuate and affects the stability of the power grid [2]. Additionally, the fluctuation of wind speed imposes higher requirements on the fatigue resistance of the main mechanical components of wind turbines [3]. Typhoons, as the main weather system that affects the working status of wind turbines, impose higher requirements for the design and selection of wind turbines. Analyzing the non-stationarity characteristics of wind speed around wind farms and its influencing factors during typhoon transit is of far-reaching significance for the refined prediction of wind power and the design of wind turbine components [4].

The non-stationarity of wind speed refers to the periodicity and fluctuation of wind speed on different time scales due to the influence of weather systems such as underlying surface characteristics, temperature, pressure, and various circulations [5–8]. Chen et al. utilized daily sounding wind data of Wuhan spanning from 1958 to 2013 to analyze the non-stationarity characteristics of annual, seasonal, and monthly mean wind speed using deviation coefficient, climate tendency rate, wavelet analysis, Yamoto mutation test, and other methods [9]. Drawing from the 1971-2015 average wind speed data of 155 meteorological stations in northern China, Han Liu et al. employed climate trend analysis, spatial interpolation, and wavelet analysis to examine the annual and seasonal spatio-temporal variation trends and periodic characteristics of the wind erosion area in northern China [10]. Understanding long-term wind change characteristics can provide early technical support for regional wind resource assessment, wind farm location, and design[11, 12]. Presently, an increasing number of studies focus on short-term wind characteristics. For instance, Chen Wenchao et al. utilized observation data from the 80m meteorological tower in Dongguan, China during Typhoon Molave, strong convection, and strong cold air events. They compared and analyzed the characteristics of three factors including 10-minute rise, average wind direction amplitude, power index of wind profile, turbulence intensity, wind attack angle, turbulence spatial integral scale, and turbulence power spectrum [13]. Similarly, Wang Hailong et al. analyzed the time-history variation characteristics of wind shear index, turbulence intensity, gust coefficient, and wind direction before and after super Typhoon "Rammasun" (No. 1409) made landfall in Xuwen, Guangdong, utilizing observation data from the Warrior Wind Farm during Rammasun's landing [14]. The study of short-term strong wind characteristics provides a theoretical basis for transmission line design, selection, and wind turbine design [15].

In the non-stationary detection of short-term wind speed, researchers often utilize linear methods such as unitary linear fitting time series and the Mann-Kendall (MK) mutation test, which can merely describe the trend characteristics of a series of time series [16]. During the period of typhoon transit, wind speed is often characterized by strong volatility. Currently, the primary methods employed to detect the non-stationarity and nonlinearity of time series changes include EMD [17], Detecting Breakpoints and Estimating Segments in Trend (DBEST), he Breaks for Additive Season and Trend Monitor (BFAST) [18], and Bayesian Estimator of Abrupt change, Seasonal change, and Trend (BEAST) [19]. EMD stands for Empirical Mode Decomposition, an adaptive signal processing method that explores local time characteristics and can address the non-stationarity trend of time series. However, when all extreme value points are included, noise increases EMD error, leading to distortion of prediction results [2]. DBEST can rapidly and reliably detect breakpoints in time series changes and accurately estimate the time and amplitude of changes, although it cannot identify changes in the period of time series [20]. The BFAST can identify long-term trends and breakpoint changes in time series, elucidating the periodic components. Similarly, BEAST can also identify long-term trends and breakpoint changes in time series, with a higher accuracy in detecting breakpoint information compared to BFAST [19]. BEAST finds widespread application in detecting surface vegetation, climate change, social ecological indicators, among others [21].

 doi:10.20944/preprints202406.0100.v1

The Hurst index is frequently employed to analyze the long-term correlation and self-similarity of wind speed in time series. Xu Zifei et al. utilized the Hurst index to analyze the time series of wind speed per minute in 2017 from a wind tower in the United States Wind Energy Research Center. Their findings revealed sharp fluctuations in wind speed and irregular monthly wind speed fluctuations, suggesting strong nonlinear characteristics [22,23].

Previous researchers have predominantly focused on studying the changing characteristics of wind speed, wind direction, and path during typhoons, as well as the temperature and precipitation caused by these storms. For instance, CAI Ju Zhen et al. analyzed the turbulent characteristics of Typhoon "Lekima" during its transit based on the 10-minute average wind speed and direction data from the Cixi Observation Station [24]. Similarly, Sun Yawen et al. analyzed the atmospheric pressure field reanalysis data of ERA5 to elucidate the precipitation mechanism in Shandong triggered by "Lekima". However, the development mechanism of the changing characteristics of wind speed during typhoons remains unexplored [25]. Studying the non-stationarity of wind speed and its influencing factors is crucial for wind power system modeling and the timely and accurate prediction of wind power. This paper addresses these issues by utilizing 15-minute wind speed and direction data from a coastal wind farm in Dafeng District, Yancheng, Jiangsu Province. The BEAST method and Hurst index analysis are applied, along with typhoon track data, surface data, and mesoscale meteorological system data, to address the following objectives:

(i) Analyzing the non-stationarity characteristics of wind speed at the measuring tower during typhoon transit using the BEAST method and Hurst index.

(ii) Investigating the causes of wind speed non-stationarity by considering factors such as wind tower wind direction, typhoon body characteristics, characteristics of the surface under the typhoon's path, and the meridional and zonal wind speed characteristics of mesoscale systems.

The remainder of this paper is organized as follows: Section 2 describes the methodology, followed by an overview of Typhoon "Likima" and its data sources in Section 3. Sections 4 and 5 present and discuss the research results in detail, and finally, Section 6 provides the conclusions.

2. Methodology

2.1. BEAST Method for Mutation Detection

BEAST is a method introduced by Zhao Kaigang in 2019 for detecting sudden change points in time series, commonly applied in detecting changes in surface conditions, climate patterns, river runoff, etc. This method employs Bayesian probability prediction, dividing the time series into three segments: seasonal signal, trend signal, and sudden change point. The calculation formula is outlined as follows [19]:

$$\hat{y}(t_i) = f(t_i;\ominus) = S(t_i;\ominus_S) + T(t_i;\ominus_T), i = 1\cdots, n \quad (1)$$

Where, ⊖S and ⊖T represent seasonal and trend signals; t is a time series.

2.2. Hurst Stationarity Analysis of Time Series

The Hurst index formula is calculated using R/S method as follows [23,26]:

(1) A time series of length N (P（t）) divide A consecutive non-overlapping subintervals of n growth $I_a(a = 1,2,\cdots,A)$, Each element of I_a is $P_{k,a}(k = 1,2,\cdots,n)$

(2) For each subinterval, calculate its standard deviation S_i, cumulative mean deviation $X_{k,a}$, and range R_i respectively:

$$S_i = \sqrt{\frac{1}{n}\sum_{k=1}^{n}(P_{k,a} - e_a)^2} \quad (2)$$

$$x_{k,a} = \sum_{i=1}^{k}(P_{i,a} - e_a) \quad (3)$$

$$R_i = \max_{1\le k\le n}(x_{k,a}) - \min_{1\le k\le n}(x_{k,a}) \quad (4)$$

Where, e_a is the mean of the I_a sequence.

(3) Calculate the (R/S) of each subinterval and the average （R/S）$_n$ of A interval n:

$$(R/S)_n = \frac{1}{A}\sum_{a=1}^{A}(R/S) \quad (5)$$

 doi:10.20944/preprints202406.0100.v1

(4) Change the subinterval in step (1) and repeat step (1) –(3) to calculate the range value for different subinterval lengths （R/S）$_n$、 lg （R/S）$_n$ and lg n there is a linear relationship, that is:

$$\lg\left(\left(\frac{R}{S}\right)_n\right) = lg\theta + Hlgn \quad (6)$$

The average range and subinterval length are plotted on the log-log coordinate plot, and the slope H is Hurst index through linear fitting by least square method.

Hurst index quantitatively describes the long-term correlation. When 0 < H < 0.5, it means that the event sequence is a long-term negative correlation, that is, if the time series shows an increasing trend in a certain interval, the following intervals are likely to decrease, and vice versa. When H≈0.5, it indicates that the time series has no long-term correlation and belongs to a non-autocorrelation random process similar to "white noise". When 0.5 < H < 1, it means that the time series is positively correlated in the long run, that is, if the time series is growing in one interval, the next interval may also grow, and vice versa.

3. Overview of Typhoon Likima and Its Data Sources

3.1. Overview of Typhoon Lekima

Super typhoon Lekima (2019) is the 5th strongest typhoon to make landfall in mainland China since 1949 [27]. On August 4, 2019, Typhoon "Lekima"(No. 201909) intensified into a tropical storm in the northwest Pacific Ocean Figure 1. Between August 4 and August 10, it swiftly moved northwestward, traversing the East China Sea, and made landfall in Wenling City, Zhejiang Province, China, as a super typhoon on August 10, boasting a central wind speed of 52m/s [28]. Subsequently, it continued northward and reached Dafeng District, Yancheng City, Jiangsu Province, passing through at 7:00 on August 11. During this time, the maximum wind speeds measured by the wind tower of a coastal wind farm in Dafeng District were 23m/s, 24m/s, 25m/s, and 19m/s at 10m, 30m, 50m, and 70m heights, respectively, over a 15-minute interval. The typhoon ultimately dissipated at 11:00 on August 13, 2019, in the Bohai Sea, China.

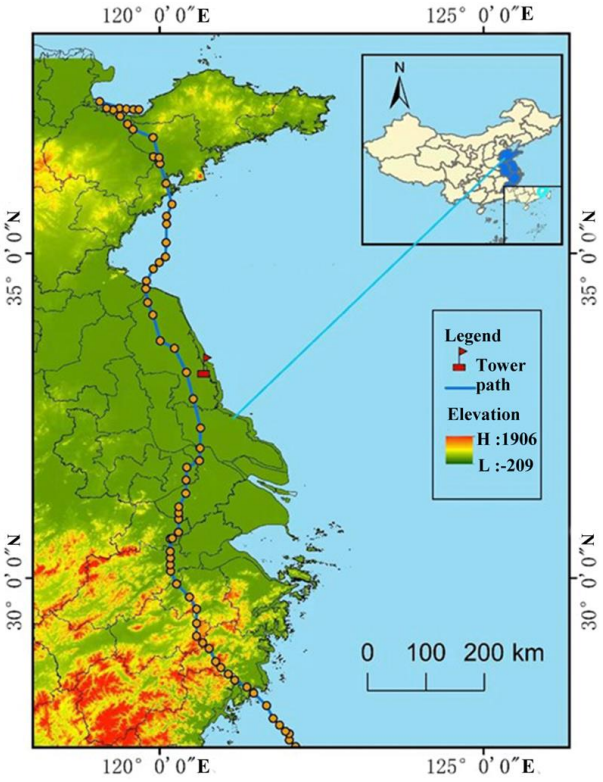

Figure 1. Overview of Typhoon Lekima.

 doi:10.20944/preprints202406.0100.v1

3.2. Data Source

In this study, wind speed and wind direction data were collected from a wind measurement tower located at coordinates (Lon. 120.7°E, Lat 33.3°N) within a coastal wind farm in Yancheng City, Jiangsu Province. Data were recorded at heights of 10m, 30m, 50m, and 70m at 15-minute intervals from August 8, 2019, 0:00 to August 13, 2019, 23:45. Missing values in the time series were interpolated using linear interpolation, followed by smoothing via a moving average technique, resulting in a complete time series of 672 data points.

Typhoon path data were obtained from the Typhoon Path Network (https://typhoon.slt.zj.gov.cn/), encompassing the position of the typhoon center, near-center air pressure, wind scale data, and the calculated distance between the wind tower and the typhoon center using ArcGIS 10.2 neighborhood analysis tools. ASTET GDEM 30m surface elevation data were retrieved from the Geospatial Data Cloud Platform (https://www.gscloud.cn). Additionally, 30m resolution land use/cover data for 2019 were downloaded from the National Ice Frozen Desert Science Data Center (https://www.ncdc.ac.cn/portal/metadata/9de270f3-b5ad-4e19-afc0-2531f3977f2f). The DEM and land use data were processed through clipping and mosaic procedures to generate a terrain and surface type map of the region traversed by the typhoon.

Furthermore, wind direction data for the mesoscale system (zonal wind U and meridional wind V) underwent reanalysis using the NCEP/DOE Reanalysis II dataset. This dataset was acquired from the US National Oceanic and Atmospheric Administration (NOAA) Physical Science Laboratory (PSL) website (https://psl.noaa.gov/data/gridded/data.ncep.reanalysis2.html).

4. Results

The BEAST method is used to detect the breakpoint information in the time series, and based on this, the start time and end time of the typhoon's influence on the wind tower are judged, and the change characteristics of time series in different stages during the typhoon's influence are analyzed. In this study, the maximum number of trend change points (Mtcp) was selected as 10 and the minimum separation interval (htcp) was selected as 96. The detection signal at the height of 10m, 30m, 50m and 70m has a good correlation with the true value, which is 0.99, 0.99, 0.98 and 0.96 respectively.

4.1. Characteristics of Wind Speed Change of Measuring Tower during Typhoon Influence Phase

4.1.1. Mutation Point Analysis of Wind Speed Sequence of Measuring Tower During Typhoon Influence Phase

According to the influence range of typhoon track and geopotential height, this paper will: At this stage, BEAST method was adopted to detect that the number of mutation points in wind speed time series at 10m, 30m, 50m and 100m of wind tower was 5, 5, 6 and 6, as shown in Figure 2. The probability values of all mutation points were maintained above 0.52. Among them, the mutation point information and probability ranking of 10m height were 324(0.99)>76(0.8)>154(0.77)>598(0.72)>407(0.62), the mutation point information and probability ranking of 30m height were 325(1.0)>76(0.98)>402(0.85)>155(0.69)>598(0.59), the mutation point information and probability ranking of 50m height were 324(1.0)=249(1.0)>428(0.95)>154(0.81)>554(0.7)=478(0.7) , the mutation point information and probability ranking of 70m height were 306(1.0)=371(1.0)=554(1.0)>160(0.95)>429(0.87)>56(0.52). It shows that the airflow field changes rapidly before and after the typhoon passes, and the stationarity of wind speed series becomes weak. In addition to the wind speed sequence at 70m height, abrupt change points appeared at 154, 324 and 598 points at 10m, 30m and 50m altitude, indicating that the time node of the typhoon really acting on the wind tower was from 154 to 598, while the abrupt change points were 56, 306 and 371 at 70m altitude, which may be due to the highest distance from the underlying surface at 70m altitude. The roughness of the underlying surface has little influence on it.

 doi:10.20944/preprints202406.0100.v1

Preprints.org (www.preprints.org) | NOT PEER-REVIEWED | Posted: 3 June 2024 doi:10.20944/preprints202406.0100.v1

4.1.2. Analysis of Series Trend of Wind Speed of Measuring Tower During Typhoon Influence Stage

According to the slope of the time series before and after the abrupt point, except for the tower with a height of 70m, the sequence can be roughly divided into two stages: intensification stage - weakening stage and strengthening stage time series; while the wind speed time series at a height of 70m can be divided into four stages: intensification - weakening - intensification - weakening. At 10m height, the slope change is 0.01-0.03-0.04-0.03-0.04-0.002; at 30m height, the slope change is 0.001-0.03-0.04—0.009-0.05-0.01. The slope change at the altitude of 50m is 0.004-0.11-0.03--0.04--0.07—0.06—0.005; the slope change at the altitude of 70m is -0.02-0.006-0.03—0.03-0.02—0.05-0. It can be seen that the wind speed at the altitude of 70m has stronger lag in response to typhoon. The air flow is less smooth.

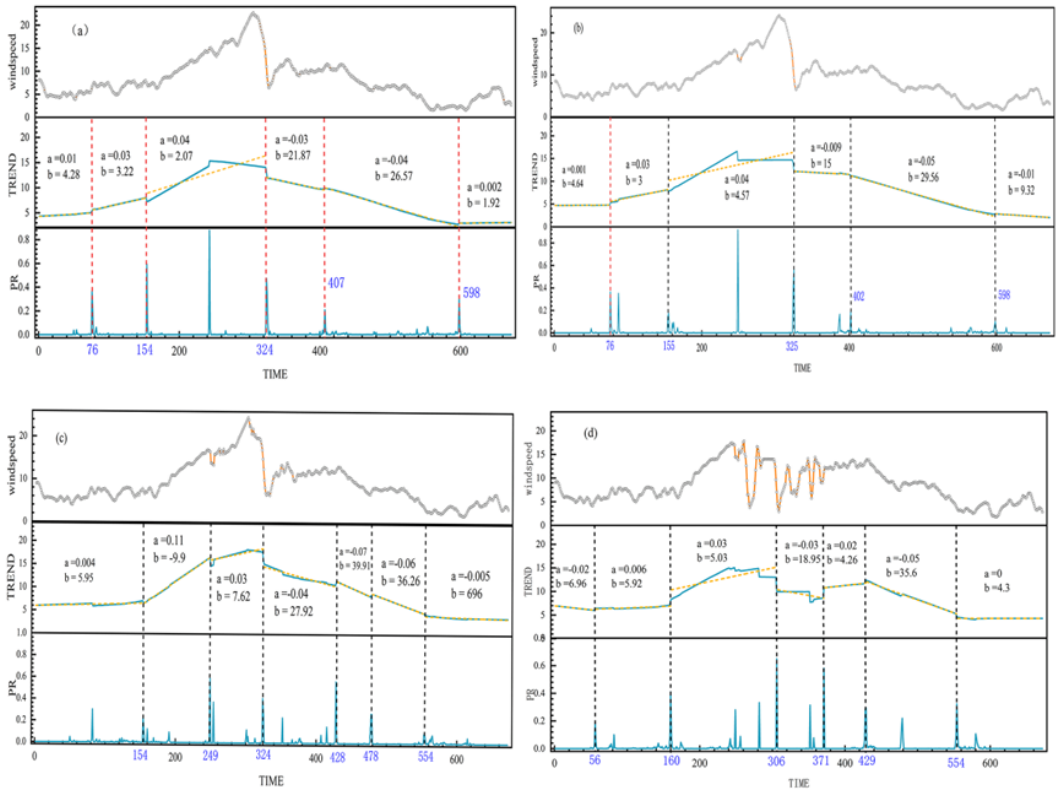

Figure 2. Beast method breakpoint detection.

Table 1. Beast point in time and probability value at the breakpoint.

CP10	TIME10	Pr10	CP30	TIME30	Pr30	CP50	TIME50	Pr50	CP700	TIME70	Pr70
76	2019/8/8 18:45	0.8	76	2019/8/8 18:45	0.98	154	2019/8/9 14:15	0.81	56	2019/8/8 13:45	0.52
154	2019/8/9 14:15	0.77	155	2019/8/9 14:30	0.69	249	2019/8/10 14:00	1	160	2019/8/9 15:45	0.95

 doi:10.20944/preprints202406.0100.v1

324	2019/8/11 8:45	0.99	325	2019/8/11 9:00	1	324	2019/8/11 8:45	1	306	2019/8/11 4:15	1
407	2019/8/12 10:00	0.62	402	2019/8/12 4:00	0.85	428	2019/8/12 10:45	0.95	371	2019/8/11 20:30	1
598	2019/8/12 5:30	0.72	598	2019/8/12 5:30	0.59	478	2019/8/12 23:15	0.7	429	2019/8/12 11:00	0.87
						554	2019/8/13 18:15	0.7	554	2019/8/13 18:15	1

4.2. Hurst Index Analysis

In summary, the wind speed time series can be segmented into two distinct stages: the strengthening stage and the weakening stage. The Hurst index is utilized to assess the smoothness of these two-time series. Specifically, the strengthening stage spans from data points 76 to 325, while the weakening stage encompasses data points 326 to 598. Based on this segmentation, the Hurst index is calculated for both stages, as illustrated in Figure 3.

During the intensification stage, the Hurst index ranges from 0.38 to 0.45, with goodness of fit R^2 values ranging from 0.88 to 0.94 across different heights of the wind measurement tower. Conversely, during the weakening stage, the Hurst index ranges from 0.36 to 0.4, with goodness of fit R^2 values ranging from 0.7 to 0.84. These results suggest that when the typhoon is active, the wind speed exhibits a Hurst index ranging from 0.38 to 0.45, with goodness of fit R^2 values between 0.8 and 0.94.

Furthermore, the wind speed time series in both the intensification and weakening stages demonstrate a pronounced long-term negative correlation. A comparison between the strengthening and weakening stages reveals that the Hurst index tends to decrease with increasing height of the wind measurement tower during the strengthening stage. Conversely, during the weakening stage, the Hurst index generally increases with height. This indicates that the self-similarity of wind speed increases with height during the strengthening stage, while it decreases with height during the weakening stage. Such trends may be attributed to variations in the airflow field before and after the passage of the typhoon.

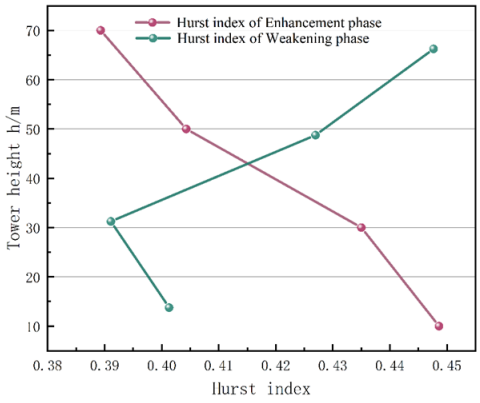

Figure 3. Hurst index calculation results.

 doi:10.20944/preprints202406.0100.v1

4.3. Analysis of Wind Direction Change Characteristics

Based on the intensification and weakening stages, the alterations in wind direction were scrutinized. As illustrated in Figure 4, throughout the duration when the measuring tower experienced the typhoon's influence, the wind direction exhibited a sequence of shifts from southeast (SE) to east (E), southeast (SE), south (S), southwest (SW), west (W), and northwest (NW). The average magnitude of these directional changes across all four altitudes was 233°, indicating Typhoon "Lekima" was within the vigorous wind zone of the eyewall.

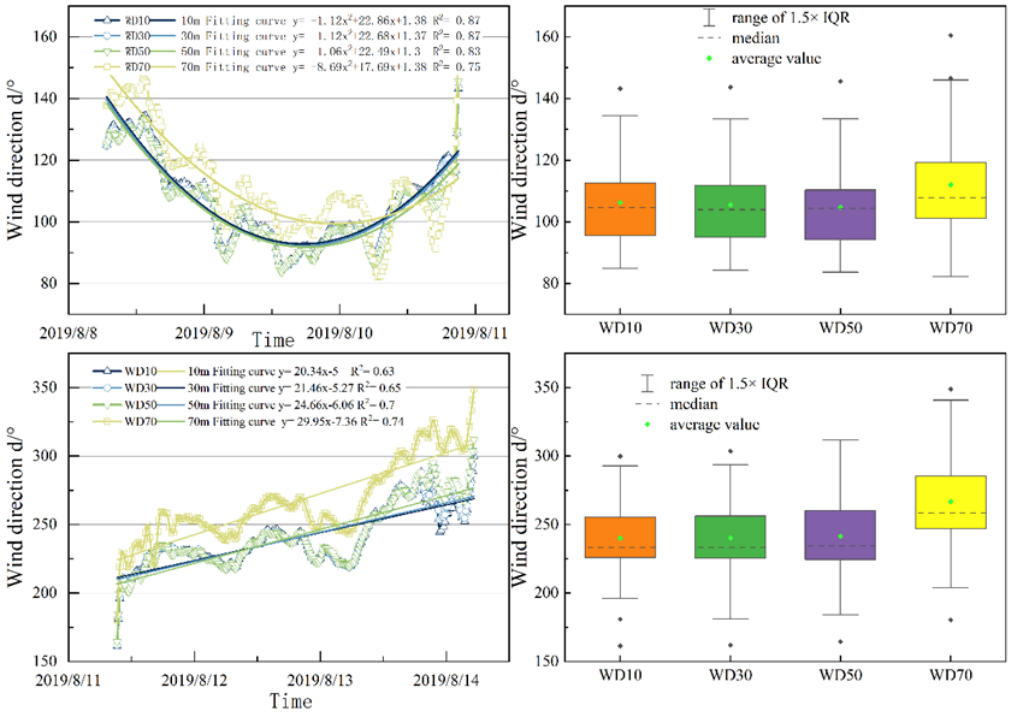

Figure 4. Wind direction variation characteristics during intensification and weakening phases.

During the intensification stage, the wind speed time series was fitted with a quadratic polynomial, yielding R^2 values exceeding 0.75 across various heights of the wind tower. Conversely, a linear fit was employed for the wind speed time series during the weakening stage, resulting in R^2 values surpassing 0.63 at different tower heights. The higher R^2 values in both stages suggest a strong fitting performance. In the intensification stage, the wind direction transitioned from southeast to east before reverting back to southeast. The fitting curves of the wind speed series at 10m, 30m, and 50m heights exhibited a high level of consistency, whereas the wind speed series curve at 70m altitude showed a distinct trend. Prior to August 20, 2019, the wind speed series curve at 70m altitude exceeded those of other altitudes, but post this time point, it fell below them. Concurrently, during the weakening stage, the wind direction swiftly shifted from southeast to southwest and ultimately to northwest. Notably, the wind direction series at 70m altitude displayed a persistently higher trend of directional change, particularly around November 9, 2019, indicating sharp alterations in the airflow field surrounding the measurement tower before and after midnight when the typhoon passed through.

Statistical analysis of wind direction during the intensification and weakening stages revealed that the mean and median wind directions at the 70m height were higher than those at other altitudes. Conversely, wind direction statistics at other altitudes exhibited similar values. This suggests that wind direction at 70m height is less influenced by underlying surface conditions and more affected by the circulation patterns of the typhoon.

 doi:10.20944/preprints202406.0100.v1

4.4. Relationship between Wind Speed Variation Characteristics and Paths at 10m and 70m

As depicted in Figure 5, the relationship between central pressure and wind speed near the typhoon center is inversely proportional—the lower the central pressure, the greater the pressure gradient between the central and surrounding areas, resulting in higher wind speeds near the center [29]. Therefore, typhoon intensity serves as a fundamental factor influencing wind speed at the wind measurement tower.

In this study, hourly wind speed data at the tower were recorded from the onset of typhoon influence until its dissipation. Analysis focused on wind speed near the typhoon center and the distance between the typhoon and the tower. Figure 5 illustrates the impact of the typhoon's body on wind speed at the tower. Before landfall, Typhoon 45 affected the tower's wind speed, despite not yet making landfall in Wenling, Zhejiang Province. The typhoon center was located at 125.10°E, 24.30°N, approximately 1088 km from the tower. The minimum central pressure was 920hPa, with a maximum wind speed near the center of 58m/s. By 7:00 on August 11, 2019, as the typhoon passed directly over the tower, its center was just 30km away, with a minimum central pressure of 982hPa and a maximum wind speed near the center of 23m/s. Even after the typhoon ceased numbering on August 13, 2019, its circulation continued to influence wind speeds at the tower. At this point, the center was positioned at 119.90°E, 37.50°N, approximately 446km from the tower, with a minimum central pressure of 990hPa and a maximum wind speed near the center of 16m/s.

During the observation period, hourly wind speeds at 10m showed a significant negative correlation with the distance between the typhoon center and the tower ($p < 0.05$, $R^2 = 0.85$), as well as with wind intensity ($p < 0.05$, $R^2 = 0.88$), indicating continued influence from the typhoon's circulation. As the typhoon center gradually moved northward, wind speeds at the tower steadily increased due to the expanding radius of the typhoon, with a significant negative correlation observed between 10m wind speed and the distance from the tower to the typhoon center ($p < 0.05$, $R^2 = 0.09$), as well as with wind intensity ($p < 0.05$, $R^2 = 0.69$). However, as the typhoon's radius diminished, wind speed at the tower became primarily influenced by local wind conditions rather than the typhoon's circulation.

In contrast, wind speed at 70m exhibited greater volatility, gradually increasing before the typhoon's passage, peaking at 17m/s around 13:00 on August 10, 2019. Subsequently, wind speed fluctuated before stabilizing. Prior to the typhoon's passage, hourly wind speed at 70m demonstrated a significant negative correlation with the distance from the typhoon to the tower ($p < 0.05$, $R^2 = 0.23$), as well as with wind intensity ($p < 0.05$, $R^2 = 0.33$). However, post-typhoon, wind speed at 70m showed no significant correlation with the distance to the typhoon ($p = 0.31$, $R^2 = 0.001$), while remaining significantly correlated with wind intensity ($p < 0.05$, $R^2 = 0.33$).

In comparison to wind speed at 10m, wind speed at 70m exhibited weaker correlations with distance from the typhoon and wind intensity both before and after its passage, indicating potential external factors influencing wind speed at this height.

 doi:10.20944/preprints202406.0100.v1

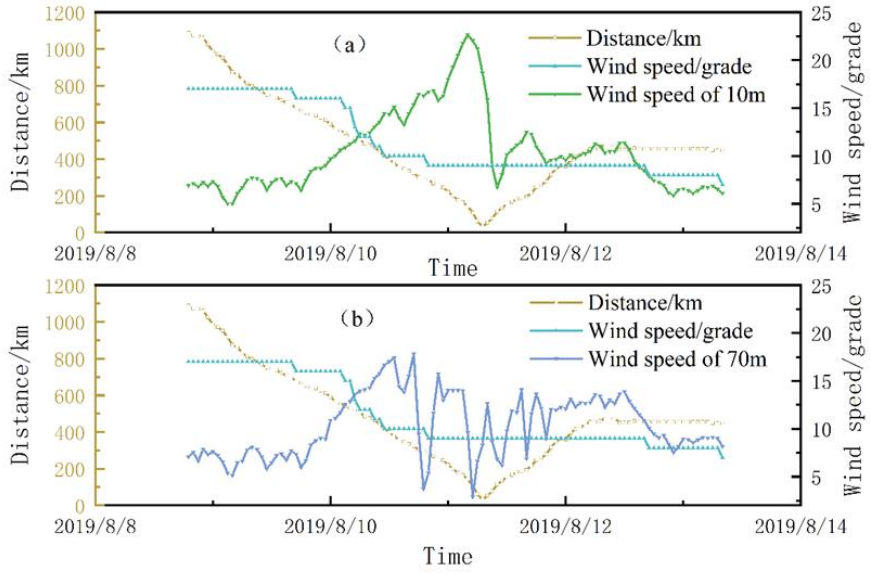

Figure 5. Influence of the cushion on the wind speed of the tower.

4.5. Influence of the Cushion on the Wind Speed of the Tower

Terrain and surface type significantly impact the intensity and trajectory of typhoons, subsequently influencing the extreme wind speeds and duration experienced by station wind towers [30]. Examining the path of Typhoon "Lijima," it traversed primarily through Zhejiang, Jiangsu, and Shandong provinces. Analyzing the terrain of these regions reveals distinct characteristics. Zhejiang's topography slopes from southwest to northeast, with mountainous terrain dominating the southwest and alluvial plains in the northeast. Notably, mountain ridges such as Dappan Mountain, Tiantai Mountain, Kuangcang Mountain, and Kuaiji Mountain align in the southwest to northeast direction, with peak elevations ranging from 1100m to 1400m. After making landfall in Wenling, Zhejiang Province, the typhoon veered northwestward, reaching the northern Zhejiang Plain within 12 hours. During this period, the central wind velocity decreased from 52m/s at landfall to 28m/s, and the typhoon's trajectory shifted from northwest to due north. While wind speeds at 10m height continued to rise, those at 70m displayed a temporary weakening trend, dropping from 17m/s to 3m/s. Additionally, wind direction fluctuations were observed at both heights, with a notable 100° larger reduction in wind direction at 70m compared to 10m.

Jiangsu, characterized by flat terrain and low average altitude, experiences a different influence from the typhoon's passage. As the typhoon moves across the northern Zhejiang Plain towards the wind tower, it traverses through the middle and lower Yangtze River Plain and the North China Plain. During this phase, spanning a linear distance of approximately 350 kilometers, the central wind speed reduces to 23m/s and maintains this speed before reaching the wind measurement tower after 15 hours. Interestingly, while wind speeds at 10m height continued to increase, those at 70m height exhibited a rising-then-decreasing pattern. Similarly, wind direction at both heights showed fluctuations, with a period of low direction at 70m. This suggests that typhoons advance more swiftly through mountainous regions with complex terrain compared to plain areas, with stronger restraining effects near their centers. Wind speeds and directions at 70m height are more influenced by large-scale typhoon circulation compared to those at 10m height.

Analyzing surface type distribution in the typhoon's transit area reveals high forest coverage in Zhejiang's mountainous regions, while the northern Zhejiang Plain and Jiangsu Plain are characterized by water systems, urban agglomerations, and farmlands. In urbanized areas like southern Jiangsu, wind tower wind speeds and directions undergo significant changes, with wind speeds at 70m height dropping to as low as 3m/s and wind direction shifting from 112° to 90°. This underscores the substantial influence of surface type on high-altitude wind speed and direction, emphasizing the lesser impact of large-scale typhoon circulation on near-surface wind characteristics.

Preprints.org (www.preprints.org) | NOT PEER-REVIEWED | Posted: 3 June 2024 doi:10.20944/preprints202406.0100.v1

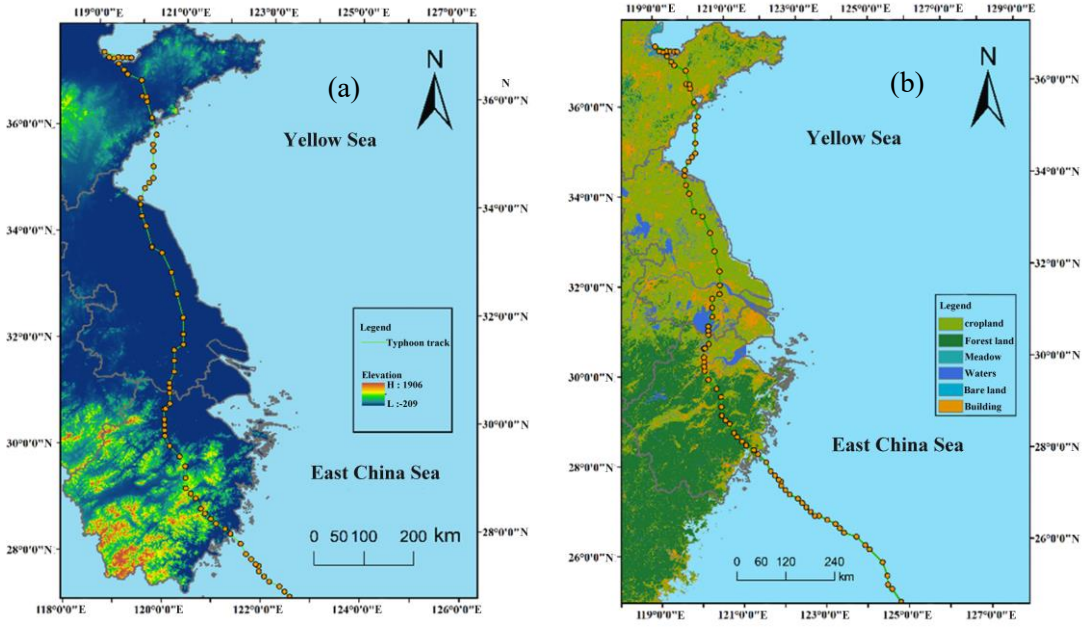

Figure 6. Typhoon track area topography and surface type.

4.6. Influence of Mesoscale System on Wind Speed of Measuring Tower before and after Typhoon

To delve into the discrepancies in wind speed and direction variation between altitudes of 10m and 70m, further analysis was conducted on the mesoscale system characteristics before and after typhoon transit, utilizing NCEP reanalysis data at a 2.5°×2.5° resolution four times a day. Focusing on the distribution of meridional (north-south) and zonal (east-west) winds U and V near the latitude and longitude (120°E, 33°N) of the wind tower, several key findings emerged [31].

Before the typhoon transit, the east-west and north-south components of Typhoon "Lechima" were balanced. Specifically, the wind measuring tower experienced influence from the easterly wind region, concentrated predominantly in the southern portion of 33°N. This easterly wind zone spanned from 600hPa to 900hPa and 25°N to 30°N in the atmosphere, and from 400hPa to 1000hPa and 30°N to 35°N at the latitude of 33°N. Notably, the position of the strong northerly wind region was comparatively lower, featuring a more stable pressure field than the easterly wind region. This stability resulted in stronger airflow disturbance at various altitude levels within the easterly wind region. Consequently, the wind direction at 70m altitude was stronger and more volatile compared to that at 10m altitude before the typhoon's passage.

Subsequent to the typhoon's transit, the westerly gale area gradually shifted southward from around 33°N. Within this gale area, wind speeds gradually decreased from 15m/s to 10m/s, and its scale expanded from 600hPa to 1000hPa down to 400 to 1000hPa. Additionally, a southerly gale area persisted south of 33°N, maintaining wind speeds at each altitude level within the range of 0-5m/s. However, the intensity of change in wind speed was smaller compared to the north-south component. Consequently, after the typhoon's passage, the wind direction at 70m altitude remained larger and more unstable than that at 10m altitude, as the wind speed experienced greater fluctuations.

5. Discussion

5.1. Comparison of BEAST Method with MK and BFAST

Wind speed data at 10m altitude underwent MK mutation testing and BFAST change point detection to delineate trend and seasonal variations in the time series data. The MK mutation test, a non-parametric statistical method, was employed to detect changes in wind speed, without imposing

 doi:10.20944/preprints202406.0100.v1

distributional assumptions on the samples [32]. Meanwhile, the BFAST method decomposed the time series into trend, seasonal, and residual components, subsequently identifying change points within the trend and seasonal components [33]. Figure 8 illustrates the outcomes of trend change detection using the MK and BFAST methods.

The results from the MK mutation test revealed that from August 8 at 5:00 to August 14 at 2:30, the UF (U statistic) value consistently exceeded 0, indicating a sustained upward trend in wind speed at 10m altitude. Although the UF and UF curves intersected at 21:45 on August 14, they failed to meet the significance level test at 0.05. On the other hand, the BFAST method identified four change points at sequences 174, 321, 442, and 549, respectively. Prior to sequence point 321, two sub-sequences (0-174, 175-321) displayed increasing trends, while sequences 550-672 exhibited an increasing trend, and 322-442, 443-549 displayed weakening trends. Despite discrepancies in the number and timing of change points between BFAST and BEAST methods, the wind speed series generally depicted both increasing and weakening trends.

The MK method, primarily suited for detecting categorical and sequential variables, may not be apt for identifying multiple mutation points [34]. In contrast, the BFAST method relies on the least squares and the minimum sliding residuals sum of squares (OLS-MOSUM) to pinpoint trend change points, selecting the optimal model based on stable regression detection estimates [35]. Conversely, the BEAST method, rooted in model space probability distribution, determines the probability value of each sample point's change according to Bayesian information principles, enabling the detection of subtle change trends [36]. The discrepancy between BFAST and BEAST change points may stem from BEAST's capacity to discern nuanced changes. However, the BFAST method necessitates manual specification of the minimum detection interval factor in parameters, possibly leading to fewer change points detected compared to the BEAST method [19].

5.2. Analysis of the Influence of Typhoon on Wind Farms and Its Measures

Preliminary analysis revealed that during the passage of Typhoon "Lekima," wind speeds at the wind farm's 10m, 30m, and 50m heights initially strengthened and then weakened, with Hurst indices indicating high non-stationarity, especially at lower heights. However, at 70m height, wind speed variations were more variable, with higher Hurst indices and significant wind direction fluctuations. Given that the wind turbine's hub height is 96m and impeller diameter is 148m, the large wind speed gradient and increased vertical wind shear during typhoons can elevate cyclic fluctuation loads on the turbine, impacting its fatigue performance and shortening its service life [37]. Sudden wind direction changes can further strain turbines with insensitive yaw systems, potentially causing blade flutter and reducing blade service life [38].

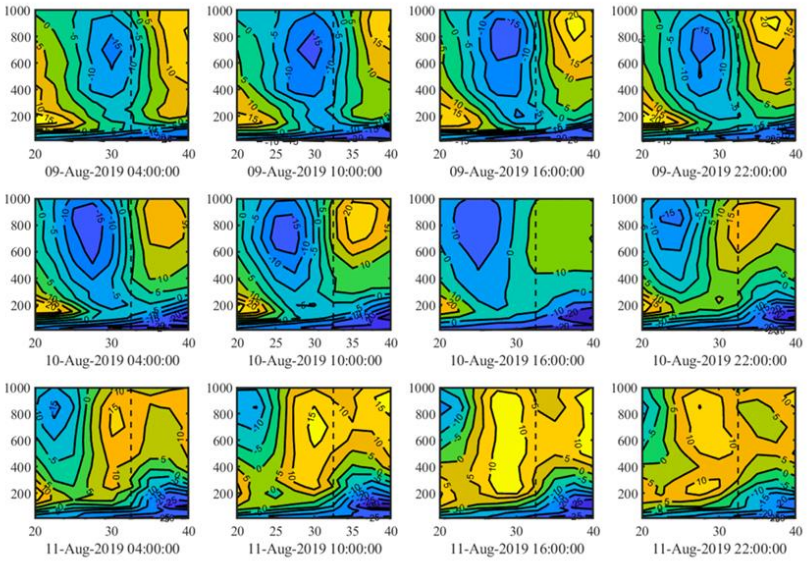

 doi:10.20944/preprints202406.0100.v1

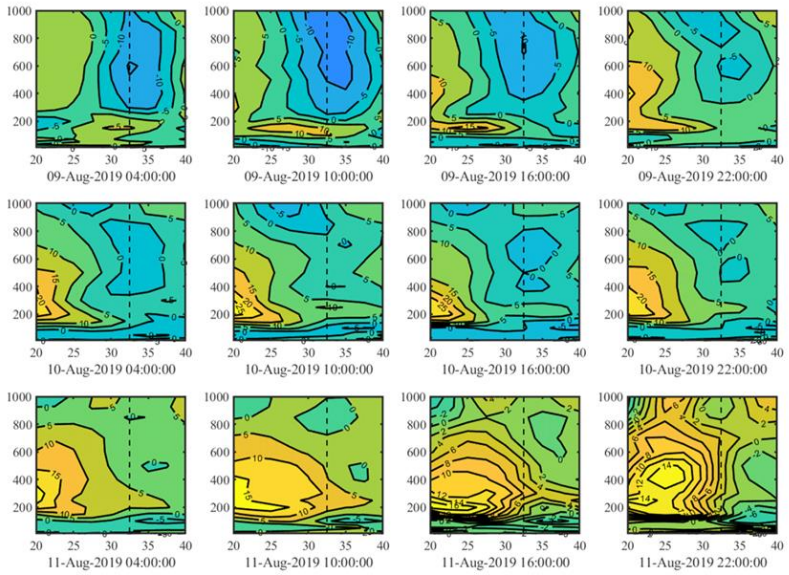

Figure 7. Profile U and V of wind speed near the tower.

Over the past decade (2012-2022), Yancheng, Jiangsu Province experienced an average of one typhoon per year, with near-central wind speeds ranging from 16m/s to 33m/s. Notably, only the 18th typhoon, "Dawei," in 2012 surpassed 25m/s wind speeds (see Figure. 8). Based on Typhoon "Lekima's" wind speed characteristics, the impact of strong winds and abrupt wind direction changes on wind turbines, and recent typhoon occurrences, the following measures are proposed:

(i) Strengthening Anti-Typhoon and Anti-Gale Early Warning Systems:

Implement an integrated intelligent supervision system across wind farms to enhance data analysis and interoperability, enabling early detection and warning of typhoon paths, wind speeds, and wind directions.

(ii) Enhancing Wind Turbine Control System Upgrades and Maintenance:

Prioritize maintenance and control system upgrades, including variable pitch, yaw, and braking systems, to mitigate typhoon damage [39]. Ensure system operability during typhoons through annual inspections and necessary upgrades.

(iii) Investing in Energy Storage Systems:

Given the region's strong economic development and electricity demand, deploy advanced energy storage technologies to address short-term power supply interruptions during typhoons [40]. These systems also support long-distance power transmission and contribute to achieving carbon reduction goals.

5.3. Deficiencies and Prospects

Based on the data of wind speed and direction at different heights of the wind tower measured every 15 minutes, this paper analyzed the change characteristics of wind speed and direction by using BFAST and Hurst index. Meanwhile, based on path characteristics, surface characteristics and mesoscale wind direction characteristics, it explored the reasons affecting the change characteristics of wind speed and direction. There are the following deficiencies:

(i) Based on the change point, this study artificially divides the wind speed and direction data of the wind tower at different heights into strengthening stage and weakening stage according to time node 325. Such division may cause the Hurst index and direction characteristic analysis to affect the judgment of the result due to the error of sample data.

(ii) In this study, typhoon body characteristics, surface characteristics and mesoscale wind direction characteristics are selected as the external characteristics that affect the wind speed and wind direction of the wind tower. In the coastal area, SST, sea and land local circulation and atmospheric circulation are also the main reasons that affect the wind speed and wind direction

Preprints.org (www.preprints.org) | NOT PEER-REVIEWED | Posted: 3 June 2024 doi:10.20944/preprints202406.0100.v1

[41], which will become one of the influencing factors for the wind speed change of the wind tower during typhoon in the future.

In extreme weather systems, higher requirements are put forward for the power prediction of wind turbines and the design of wind turbines. In this paper, the characteristics and influencing factors of wind speed and direction change of wind tower in wind farms are studied in order to further study the wind power prediction model in the future.

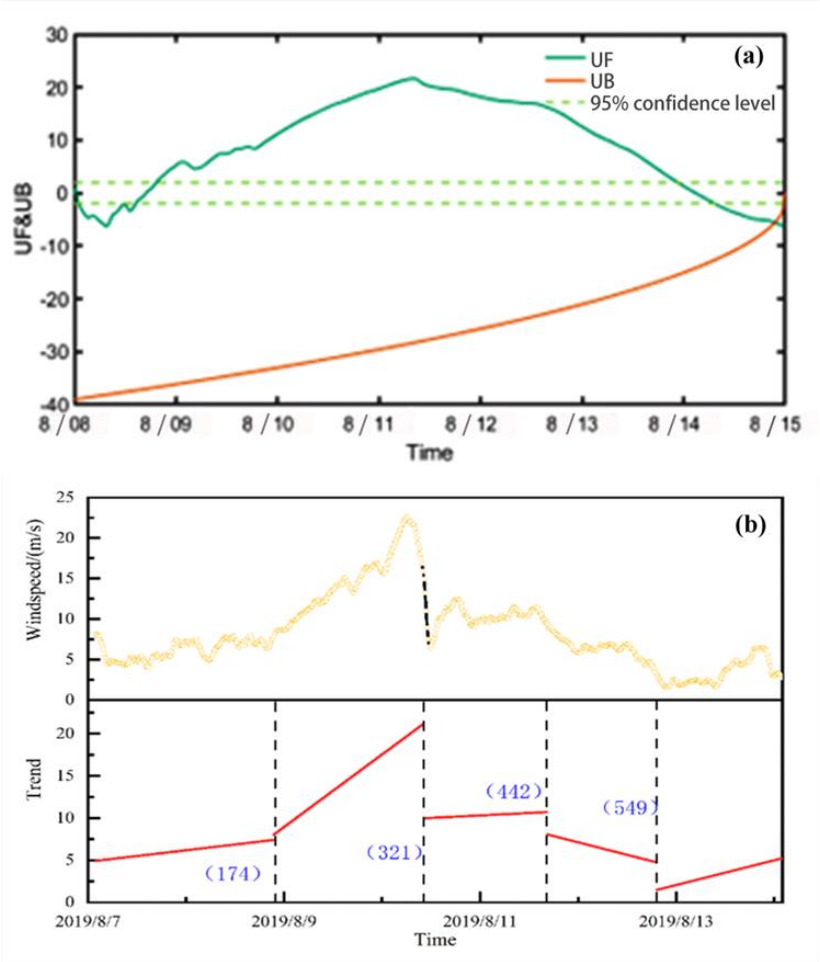

Figure 8. MK and BFAST change detection methods.

6. Conclusion

Based on wind speed and wind direction data at 10m, 30m, 50m and 70m heights of a wind power tower in Yancheng, Jiangsu Province, this paper analyzes the change characteristics of wind speed and wind direction by using BFAST method and Hurst index. Based on typhoon body data, topographic data and mesoscale system wind direction data, the causes of the occurrence and development of wind speed and wind direction of wind tower are further analyzed, and a conclusion is drawn:

(i) In BFAST method, there are 5, 5, 6 and 6 change points at the height of 10m, 30m, 50m and 70m respectively. Among them, the change points at the height of 10m, 30m and 50m all change before and after node 325, while the change time point at the height of 70m is inconsistent with other heights. Hurst index results show that the non-stationarity of wind speed series at 70m altitude is stronger than that at other altitudes.

(ii) The wind direction sequence at the height of 10m, 30m, 50m and 70m was fitted by stages. It was found that the direction of wind direction was SE-E-SE-SW-W-NW. Among them, the trend line

 doi:10.20944/preprints202406.0100.v1

fitted at the height of 70m had a large deviation from other altitudes at the wind speed strengthening and weakening stages.

(iii) The wind speed at the height of 10m and 70m has different response degrees to the typhoon body. The correlation between the wind speed and the distance between the wind measurement tower and the typhoon near the center is stronger at the height of 10m than at the height of 70m. The surface type and the wind direction of the mesoscale system also have certain effects on the wind speed and direction.

In this paper, the change characteristics and influencing factors of wind speed and direction of wind tower are studied, which provides methods and theoretical support for the study of short-term wind speed when typhoon passes through and provides reliable support for the selection of wind power forecast indicators and the selection and design of wind turbines under extreme gale weather systems.

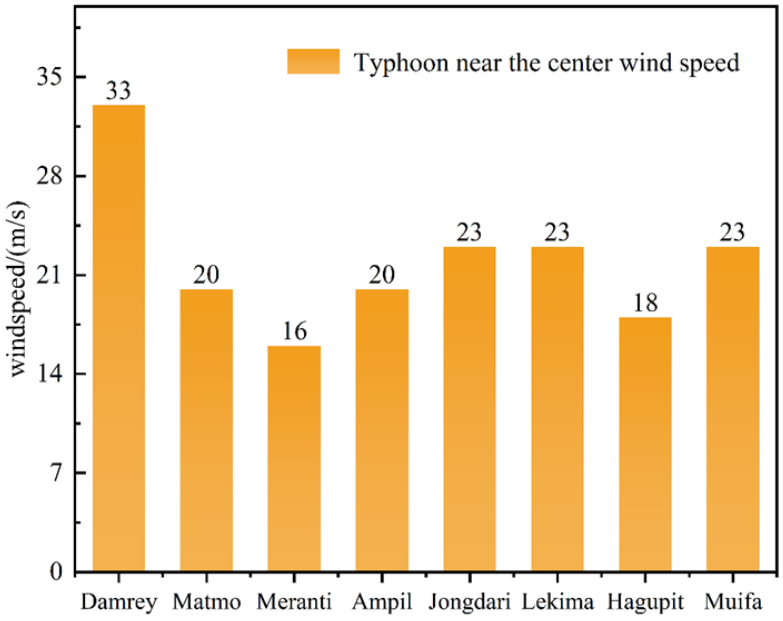

Figure 9. Transit tower typhoon over the years.

Author Contributions: The authors confirm contribution to the paper as follows: study conception and design: Wenzheng Yu; data collection: Haibo Sheng; analysis and interpretation of results: Aodi Fu; draft manuscript preparation: Lingzi Wang. Liyuan Deng. Weisi Deng. All authors reviewed the results and approved the final version of the manuscript. Conceptualization, L.W., and A.F.; methodology, L.W.; software, L.W; validation, L.W., A.F. and J.G.; formal analysis, A.F.; investigation, W.Y.; resources, L.W., A.F. and Y.Z.; data curation, H.S.; writing—original draft preparation, L.W., L.D., and W.D.; writing—review and editing, J.G., B.B, and K.A., visualization, L.W., A.F.; supervision, K.A.; project administration, H.S.; funding acquisition, B.B. All authors have read and agreed to the published version of the manuscript.

Funding: This work was supported by the new power system technology project of China Southern Power Grid Corporation (000000KK52210138), authors is Lingzi Wang, and the Second Tibet Plateau Scientific Expedition and Research Program (STEP) under grant number 2019QZKK0804, (Wenzheng Yu). And this work also was supported by the Researchers Supporting Project, grant number (RSP2024R296), King Saud University, Riyadh, Saudi Arabia.

Data Availability Statement: The data presented in this study are available upon request from the corresponding authors.

Acknowledgments: We would like to thank China Southern Power Grid Company's New Power System Technology Project (000000KK52210138) and the Second Qinghai-Tibet Plateau Scientific Investigation and Research Program (Approval number :2019QZKK0804) for providing funding for this research, and Jiangsu

 doi:10.20944/preprints202406.0100.v1

Haihailongyuan Wind Power Co., Ltd. for providing wind speed and direction data. Thank you to everyone who contributed to the study.

Conflicts of Interest: The authors declare that they have no conflicts of interest to report regarding the present study.

References

1. Sahu, B. K. (2018). Wind energy developments and policies in China: A short review. Renewable and Sustainable energy reviews, 81, 1393-1405.
2. Chen, Y., Zhang, D., Qi, W. (2023). Power prediction of a Savonius wind turbine cluster considering wind direction characteristics on three sites. Journal of Cleaner Production, 423, 138789.
3. Tao, T., Long, K., Yang, T. (2023). Quantitative assessment on fatigue damage induced by wake effect and yaw misalignment for floating offshore wind turbines. Ocean Engineering, 288, 116004.
4. Wang, H., Wang, T., Ke, S. (2023). Assessing code-based design wind loads for offshore wind turbines in China against typhoons. Renewable Energy, 212, 669-82 (In Chinese).
5. Duan, J., Zhang, L., Xie, Z. N. (2022). Study on non-stationary wind characteristics of mangosteen Typhoon. Journal of Vibration and Shock, 41,18-26 (In Chinese).
6. Hui, Y., Li, B., Kawai, H. (2017). Non-stationary and non-Gaussian characteristics of wind speeds. Wind and Structures, 24(1), 59-78.
7. Qin, Z. Q., Xia, D. D., Dai, L. M. (2022). Investigations on Wind Characteristics for Typhoon and Monsoon Wind Speeds Based on Both Stationary and Non-Stationary Models. Atmosphere, 13(2).
8. Mahrt, L., Nilsson, E., Rutgersson, A. (2020). Sea-Surface Stress Driven by Small-Scale Non-stationary Winds. Boundary-Layer Meteorology, 176(1), 13-33.
9. Chen, C., Meng, D. (2015). Variation characteristics of low altitude wind speed in Wuhan City from 1958 to 2013. Resources and Environment in the Yangtze Basin, 24, 30-7 (In Chinese).
10. Han, L., Wang, J. P., Wang, G. Z. (2018). Temporal and spatial characteristics of wind speed variation in the wind erosion area of northern China. Arid Land Geography, 41, 963-71 (In Chinese).
11. Xu,J., Hu, Y.Z., Li, J.X. Analysis Of Long-Term Wind Speed Trends And Assessment Of Wind Resources In China Sea Area Under The Background Of Global Warming. Advances in Marine Science, 1-12 (In Chinese).
12. Zhao, L., Wei, C., Wang, Y. Macro Location Of Offshore Wind Farms And Estimation Of Wind Energy Resources Reserves. Acta Energiae Solaris Sinica, 1-7 (In Chinese).
13. Chen, W. C., Liu, A. J., Song, L. L. (2019). A case study of wind characteristics of different strong wind weather systems. Meteorological Monthly, 45 ,251-62 (In Chinese).
14. Wang, H. L., Wu, X. Q., Huang. H. Z. (2018). Analysis of variation characteristics of near-ground wind speed during the landing of super Typhoon Rammasun. Journal of Tropical Meteorology, 34, 297-304 (In Chinese).
15. Wei,X.W., Qiu, X.Y.,Li, X.Y. (2010). Multi-objective reactive power optimization of power grid including wind farm. Power System Protection and Control, 38(17), 107-11 (In Chinese).
16. Jiang, S., Xu, P. P., Li, X. (2022). Study on the conversion coefficient of wind speed at different elevations and the variation characteristics of wind speed at higher elevations in offshore wind farms. Power Systems and Big Data, 25, 52-9 (In Chinese).
17. Huang, J., Yu, H., Guan, X. (2016). Accelerated dryland expansion under climate change. Nature Climate Change, 6(2), 166-71.

 doi:10.20944/preprints202406.0100.v1

18. Verbesselt. J., Hyndman, R., Newnham, G. (2010). Detecting trend and seasonal changes in satellite image time series. Remote Sensing of Environment, 114(1), 106-15.
19. Zhao, K., Wulder, M. A., Hu, T. (2019). Detecting change-point, trend, and seasonality in satellite time series data to track abrupt changes and nonlinear dynamics: A Bayesian ensemble algorithm. Remote Sensing of Environment, 232.
20. Fang, X., Zhu, Q., Ren, L. (2018). Large-scale detection of vegetation dynamics and their potential drivers using MODIS images and BFAST: A case study in Quebec, Canada. Remote Sensing of Environment, 206, 391-402.
21. DELLICOUR S, GILL M S, FARIA N R, et al. Relax, Keep Walking - A Practical Guide to Continuous Phylogeographic Inference with BEAST [J]. MOLECULAR BIOLOGY AND EVOLUTION, 2021, 38(8): 3486-93.
22. Yuan, Q. Y., Yang, Y., Li, C. (2018). Research on wind speed time series based on Hurst index. Applied Mathematics and Mechanics, 39, 798-810 (In Chinese).
23. Xu, Z. F., Zou, J. H., Li, C. (2019). Hurst index analysis of wind speed time series based on R/S class analysis. Applied Mathematics and Mechanics, 39, 585-90+604 (In Chinese).
24. Cai, J. Z., Xu, J. Y., Shao, X. (2021). Analysis of wind field and turbulence characteristics of Typhoon Lichima. Journal of Nanjing University(Natural Science), 57, 896-903 (In Chinese).
25. Sun, Y. W., Fu, D., Wang, B. (2023). Cause analysis of precipitation caused by Typhoon "Lekima" in Shandong Province. Transactions of Oceanology and Limnology, 45, 17-22 (In Chinese).
26. Wang, Y. Z., Li, B., Wang, R. Q. (2011). Application of the Hurst exponent in ecology. Computers & Mathematics With Applications. 61(8), 2129-31.
27. Gao, Y., Zhang, Y., Lei, L., & Tang, J. (2023). Multi-scale characteristics of an extreme rain event in Shandong Province, produced by Typhoon Lekima (2019). Frontiers in Earth Science, 10, 1093545.
28. Li, X.X., Zhang, Y.X., Cao, X.Z. (2023). Analysis of SST variation characteristics of Typhoon Lekima (1909). Chinese Journal of Atmospheric Sciences. 47(05), 1295-308 (In Chinese).
29. Lin, Q. H., Ding, S. (2024). Analysis of Typhoon-Induced Wind Fields in Ports of the Central and Northern Taiwan Strait. Sustainability. 16(1).
30. Petrovic, P., Romanic, D., Curic, M. (2018), Homogeneity analysis of wind data from 213 m high Cabauw tower. International Journal Of Climatology. 38, E1076-E90.
31. Huang, W. F., Xu, Y. L., Li, C. W. (2011). Prediction of design typhoon wind speeds and profiles using refined typhoon wind field model. Advanced Steel Construction. 7(4), 387-402.
32. Zhang, C. Y., Peng, L. (2017). Analysis on variation characteristics of wind direction and speed in Hongjia meteorological Station from 1981 to 2010. Journal of Meteorological Research and Application, 38, 72-6+115 (In Chinese).
33. Hu, D. (2017). GPS time series is analyzed by BFAST algorithm (Ph.D. Thesis). Southwest Jiaotong University, Chengdu.
34. Liu, X. W., Xu, Z. X. (2020). Spatial and temporal pattern of extreme temperature during 1961-2018 in China. Journal Of Water And Climate Change. 11(4), 1633-44.
35. Mendes, M. P., Rodriguez-Galiano, V., Aragones, D. (2022). Evaluating the BFAST method to detect and characterise changing trends in water time series: A case study on the impact of droughts on the Mediterranean climate. Science Of The Total Environment. 846.
36. Gill, M. S., Lemey, P., Suchard, M. A. (2020). Online Bayesian Phylodynamic Inference in BEAST with Application to Epidemic Reconstruction. Molecular Biology and Evolution. 37(6), 1832-42.

 doi:10.20944/preprints202406.0100.v1

37. Jia, Y. Y. (2018). Study on the operation of offshore wind turbines, typhoon aerodynamic performance and wake field characteristics (Ph.D. Thesis). Tianjin University, Tianjin.
38. He, G. L., Tian, J. K., Chang, D. S. (2013). Typhoon resistance concept design of offshore wind turbine. Electric Power Construction, 34, 11-7 (In Chinese).
39. Liu, J., Zhang, Z. Q., Gan, Q.Y. Optimal control of independent variable pitch of wind turbine based on random disturbance correction. Control Theory & Applications, 1-7 (In Chinese).
40. Tang, J., Yue, F., Wang, L.X. (2024). Global new energy storage technology development situation analysis. Journal of Global Energy Interconnection, 7(02), 228-40 (In Chinese).
41. Qiu, X. N., Fan, S. J. (2013). Application of the data of automatic weather station in the study of local circulation such as sea and land winds. Acta Scientiarum Naturalium Universitatis Sunyatseni, 52, 133-6 (In Chinese).